Intra-ply, inter-ply and FG hybrid composites based on basalt and poly-ester fibers: Flexural and impact properties

Ehsan Fadayee Fard[1], Hassan Sharifi[*1], Majid Tehrani[**2] and Ehsan Akbari[1]

[1]Department of Materials Science, Faculty of Engineering, Shahrekord University, Shahrekord, Iran
[2]Department of Art, Shahrekord University, Shahrekord 56811-88617, Iran

Abstract.   Basalt and poly-ester fibers along with epoxy resin were used to produce inter-ply, intra-ply and functionally gradient hybrid composites. In all of the composites, the relative content of basalt fiber to poly-ester fiber was equal to 50 percent. The flexural and charpy impact properties of the hybrid composites are presented with particular regard to the effects of the hybrid types, stacking sequence of the plies, loading direction and loading speed. The results show that with properly choosing the composition and the stacking sequence of the plies; the inter-ply hybrid composites can achieve better flexural strength and impact absorption energy compared to the intra-ply and functionally gradient composites. The flexural strength and impact absorption energy of the functionally gradient hybrid composites is comparable to, or higher than the intra-ply sample. Also, by increasing the loading speed, the flexural strength increases while the flexural modulus does not have any special trend.

1. Introduction

   In the past decades, the development of fiber reinforcing composites has been growing rapidly due to their unique characteristics in different industries. The great properties of these composites can be due to their high strength to weight ratio, heterogeneous properties, excellent environmental resistance, fatigue resistance and high durability (Rajak *et al.* 2019).

   Nowadays, the main reinforcing materials for structural polymer composites are glass and carbon fibers. It has been proved in the last few years that, due to the disadvantages of these two conventional reinforcing fibers, there is a demand for the new types of fibers to be introduced. As a result of intensive scientific research around the world, the use of natural and environmental friendly fibers such as basalt fiber has been proposed. Basalt fibers have higher strength and modulus and are also more heat and chemical resistant especially in alkaline environments compared to the glass fibers (Lopresto *et al.* 2011, Azizi and Eslami-Farsani 2021, Kim *et al.* 2019). Moreover, basalt fibers, due to their reasonable price, are often preferred over carbon fibers,

---

∗Corresponding author, Associate Professor, E-mail: sharifi@sku.ac.ir
∗∗Co-corresponding author, Associate Professor, E-mail: mtehrani@sku.ac.ir

which are chemically neutral and considered as high strength fibers (ArySubagia and Kim 2013, Artemenko 2003). Due to the lack of information on basalt fibers and their composites, further research is needed to elucidate their mechanical and chemical properties.

In spite of the advantages, polymer composites also have some problems with metals. Composites which are reinforced with brittle fiber, such as carbon or basalt, can be damaged under impact or bending loads. These damages can reduce the mechanical properties of the composites including the tensile, compressive, fatigue and flexural strength. In some cases, damages which are not even visible by eye can reduce the compressive strength up to 50 percent (Sun and Hallett 2017, Onal and Adanur 2019, Caminero *et al. 2018*). On the other hand, composites which are reinforced with ductile fiber such as nylon or poly-ester (PE) have good impact properties but they do not have good tensile, compressive and flexural properties (Nosraty *et al.* 2015). To solve this problem, researchers have proposed various solutions, including hybrid composites in combination with brittle and ductile reinforcements. By using brittle and ductile fibers in one matrix; advantages of these two fibers are obtained (Tehrani *et al.* 2010, Pegoretti *et al.* 2004, Hancox 1981).

Hybrid composites are made by combining two or more fibers of different types. Depending on the geometric pattern of the fiber arrangements, they may be classified as inter-ply hybrids, where layers of the two (or more) homogeneous reinforcements are stacked, and intra-ply hybrids where two (or more) constituent types of fibers are mixed in the same layer (Ozbek *et al.* 2019, Pegoretti *et al.* 2004). With combination of intra-ply and inter-ply methods, the third class of hybrid composites called functionally gradient material (FGM) have been proposed.

In the recent years, there has been growing interest in the use of FGMs due to their numerous advantages over composite materials. Owing to the graded variation in the composition, the properties of FGMs change significantly and continuously from one surface to another, thus eliminating the interface problems like stress concentrations and poor adhesion (Bharti *et al.* 2013). Depending upon the nature of the gradient, the FGMs (composites) may be classified as fraction gradient, size gradient, shape gradient and orientation gradient type. The application of FGMs is increasing in aerospace, defense, nuclear industry, biomedical and electronics sectors (Bharti *et al.* 2013, Thomas and Roy 2016).

The mechanical behavior of polymer composites which are reinforced with one type of fiber and with a FGM structure have been studied by many researchers such as Lee (1997), Huang (2002) and Bafekrpour (2013). In recent years the concept of FGM has been extended to the field of polymer-reinforced composites with more than one type of fiber (hybrid composites). FGM-based hybrid composites have at least two types of reinforcement and the proportion of one reinforcing fiber to another, from the top layer to the bottom layer gradually increases (Jang and Lee 1998). Due to the difficulties of producing FGM type of hybrid composites, the mechanical behavior of these composites has been investigated in a few studies. Jang and Lee (1998) investigated on the flexural and instrumented impact properties of the two kinds of FGMs. These composites were fabricated by changing the spatial distribution of glass fiber and carbon fiber in poly-phenylene sulfide matrix.

Our investigation on the previous studies showed that, the research on FGM hybrid composites have not been performed extensively, and some functional gradients reported recently have been made only by the spatial distribution of one reinforcing fiber in the composites. In this study, the mechanical properties of basalt/PE-epoxy functionally gradient composites as a function of spatial distribution of the reinforcing fibers are measured. The effect of spatial distribution and loading speed on the flexural and charpy impact properties is investigated and compared with the intra-ply

Table 1 Properties of the used basalt, PE fibers and epoxy resin

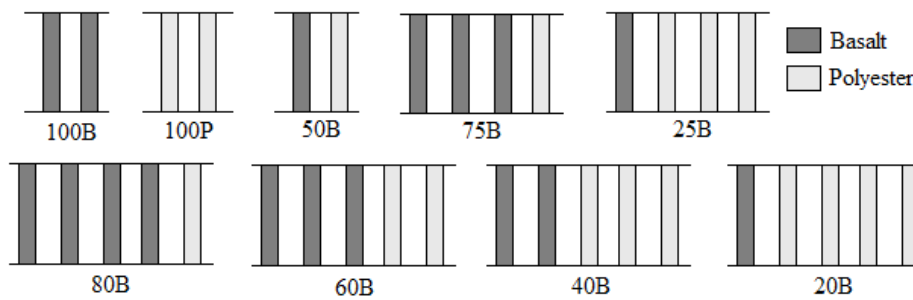| Properties	Basalt	PE	Epoxy
Density (kg/m^{-3})	2700	1120	1110
Tensile modulus (GPa)	85	4.05	2.78
Tensile strength (MPa)	1800	284	75
Strain at break (%)	2	6.9	2

Fig. 1 Schematic view of the used reinforcements with different contents of basalt and PE fibers

and inter-ply hybrid composites. In addition, scanning electron microscopy (SEM) analysis was used to determine the extent and type of the damage in the tested specimens. The results of this research may be utilized in designing sports equipment and in constructions of aircraft and cars.

2. Experimental procedure

2.1 Materials and specimen preparation

In this study, basalt and PE fibers were used as reinforcing fibers. The basalt fiber was supplied by Hengdian Group Shanghai Russia and Gold Basalt Fiber Co. (China) in the form of 800 Tex. The PE fiber was supplied by Zhejiang Guxiandao Industrial Fiber Co. (China) in the form of 337 Tex. These fibers were supplied with a suitable size for using with epoxy resin. The thermo-set resin used in this study was epoxy, ML-506 grade produced by Mokarrar Co., Iran. The properties of the two fibers and epoxy resin are presented in Table 1.

The required reinforcements were prepared with a unidirectional structure and 5 ends/cm counts. Nine different types of reinforcement were produced, namely; pure basalt, pure PE and seven mixtures of basalt and PE with different volume percentages of basalt fiber. In Fig. 1 the composition of each of the reinforcements is shown in more detail. In this figure, reinforcements were coded by using the percentage of the basalt and PE fibers. For example, sample 80B has 80 percent basalt fiber and 20 percent PE fiber.

All of the composites were made by hand lay-up method. Three types of laminates were obtained: inter-ply, intra-ply and FGM hybrids. In FGM specimens, relative volume fraction of basalt fibers to PE fibers is 100 percent at the top layer and it decreases linearly to zero percent until the bottom layer is reached or vice versa. In all of the hybrid composites, the relative content of basalt fibers to PE fibers is equal to 50 percent. The composites consisted of 12-ply laminates with the cross-ply stacking sequence ($[0/90]_{3s}$). All of the laminates were cured for 3 hours at

Table 2 Thickness, fiber volume fraction and experimental density of the prepared laminates

Laminate code	Layer arrangement	Thickness (mm)	Volume fraction (%)	Experimental density (kg.m^{-3})
Interply1f	[(100B/100B), (100B/100B), (100B/100B), (100P/100P), (100P/100P), (100P/100P)]	3.95	46	1443
Interply1b	[(100P/100P), (100P/100P), (100P/100P), (100B/100B), (100B/100B), (100B/100B)]	3.95	46	1443
Interply2f	[(100B/100B), (100P/100P), (100B/100B), (100P/100P), (100B/100B), (100P/100P)]	3.96	46	1447
Interply2b	[(100P/100P), (100B/100B), (100P/100P), (100B/100B), (100P/100P), (100B/100B)]	3.96	46	1447
Intraply	[(50B/50B), (50B/50B), (50B/50B), (50B/50B), (50B/50B), (50B/50B)]	3.96	46	1372
FGM1f	[(100B/100B), (80B/80B), (60B/60B), (40B/40B), (20B/20B), (100P/100P)]	3.51	52	1441
FGM1b	[(100P/100P), (20B/20B), (40B/40B), (60B/60B), (80B/80B), (100B/100B)]	3.51	52	1441
FGM2f	[(100B/100B), (75B/75B), (50B/50B), (50B/50B), (25B/25B), (100P/100P)]	3.57	51	1433
FGM2b	[(100P/100P), (25B/25B), (50B/50B), (50B/50B), (75B/75B), (100B/100B)]	3.57	51	1433
FGM3f	[(100B/100B), (50B/50B), (50B/50B), (50B/50B), (50B/50B), (100P/100P)]	3.79	48	1411
FGM3b	[(100P/100P), (50B/50B), (50B/50B), (50B/50B), (50B/50B), (100B/100B)]	3.79	48	1411

40°C, followed by 1 hour at 80°C under a constant pressure. Then the composites were allowed to slowly cool down to room temperature under pressure. The layer arrangement, average thickness, volume fraction of the fibers and the experimental density of the prepared laminates are reported in Table 2.

2.2 Mechanical tests

To evaluate the mechanical properties of the inter-ply, intra-ply and FGM composites, flexural and impact tests were performed. The method for preparing specimens and mechanical testing were based on the American Society for Testing Material (ASTM) standards; ASTM D.790-03 (2003) for three-point bending tests and ASTM D.256 (2018) for the charpy impact tests. The dimension of the flexural test specimens was 100 mm×25 mm. The support span was fixed at 50 mm, and the test was performed under crosshead speeds of 1.3, 10 and 100 mm/min. Four specimens per each case were tested using a Hounsfield, H25Ks equipped with a 25 kN load cell. From the basic force-deflection curves, important parameters such as flexural strength and flexural modulus were calculated bythe following equations (2003)

$$\sigma_f = 3PL/2bd^2 \tag{1}$$

$$E_B = L^3m/4bd^3 \tag{2}$$

Where σ_f is the flexural strength (MPa), P is the maximum load (N), L is the support span

(mm), *b* and *d* are the width and thickness of the samples (mm) and *m* is the slope of the tangent to the initial straight-line portion of the load-deflection curve (N/mm).

The dimension of the charpy impact specimens was 80 mm×10 mm. All of the samples were tested by using a Zwick, D-7900 tester. Five specimens per each case were tested and the absorbed energy was recorded after the impact. To normalize the obtained impact absorption energies they were divided by the cross-sectional area of the specimens.

2.3 Scanning electron microscopy (SEM)

SEM analysis was performed on a large number of flexural and impact test samples to determine the actual failure mechanisms. The microstructure of the samples was studied using a Philips (model XL30, Netherlands) scanning electron microscope. Prior to all SEM observations, the specimens were sputtered with gold to prevent charging. The samples were viewed through the surface and cross section area.

2.4 Statistical analysis

The results of the flexural and impact tests are reported as mean and standard deviation. One-way analysis of variance (ANOVA) was used to compare the flexural and impact parameters between the inter-ply, intra-ply and FGM laminates. A P-value<0.05 was considered as a significant value.

3. Results and discussion

3.1 Flexural properties

3.1.1 Flexural properties as a function of hybridization type and the sequence of the stacking plies

Figs. 2(a)-(c) show the stress/deflection curves for the inter-ply, intra-ply and FGM composites at loading speeds of 1.3, 10 and 100 mm/min under bending. The results show that, the flexural behavior of the hybrid composites change markedly when the spatial distributions of the reinforcing fibers are altered in the hybrids. The spatial distribution of the reinforcing fibers has an effect on the relative locations of the different kinds of the fibers across the thickness of the laminate.

The results of Figs. 2 (a)-(c) show that especially after the maximum stress point, the flexural behavior of the Interply2f specimen is significantly different from the other specimens. In the elastic region, it can be seen that, the Interply2f specimen shows the highest maximum stress, initial steep slope, and low deflection at maximum stress. This behavior is due to the stacking sequence of this sample. In this sample, the presence of full basalt layers all over the thickness of the specimen caused the specimen to withstand tensile and compressive stresses in the lower and upper layers, respectively. Failure in this specimen occurred unlike the other specimens in two stages and abruptly after the maximum stress point. In this specimen at a deflection of about 4.6 mm, the primary failure occurred due to the rupture of the basalt fiber, but the presence of the basalt fiber-rich layer in the tensile side prevented the overall collapse of the specimen and withstanding a tensile strength up to about 6.3 (up to 7.5 at different loading speeds) deflection. At
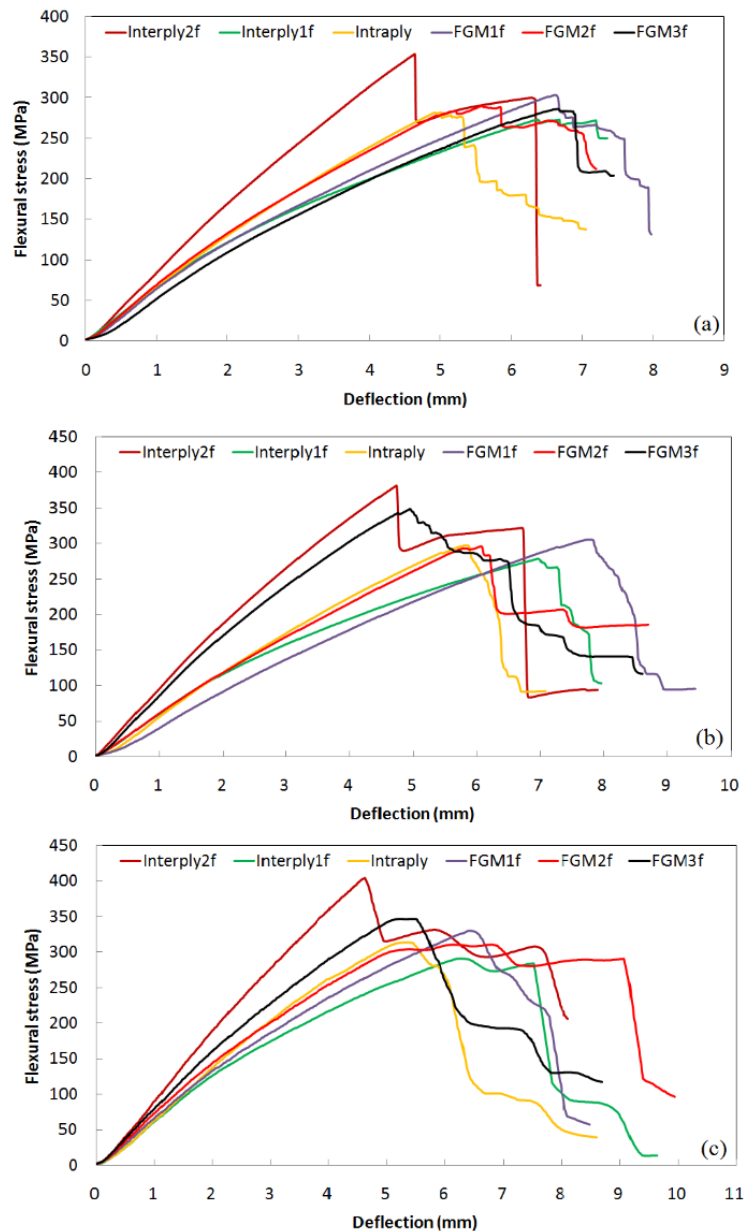
Fig. 2 Flexural stress/deflection of different hybrid laminates at (a) 1.3, (b) 10 and (c) 100 mm/min

this point, fracture occurred abruptly due to the rupture of the lower basalt layers.

After the end of the elastic region, it can be seen that the other specimens had a progressive failure (especially at 1.3 and 10 mm/min loading speed). At 100 mm/min loading speed, the stress decreases drastically in samples of Intraply and FGM3f, while in the other samples the stress decreases gradually. At all loading speeds, the stress drop is associated with the delamination, debonding of PE fibers and failure of the matrix and basalt fibers.
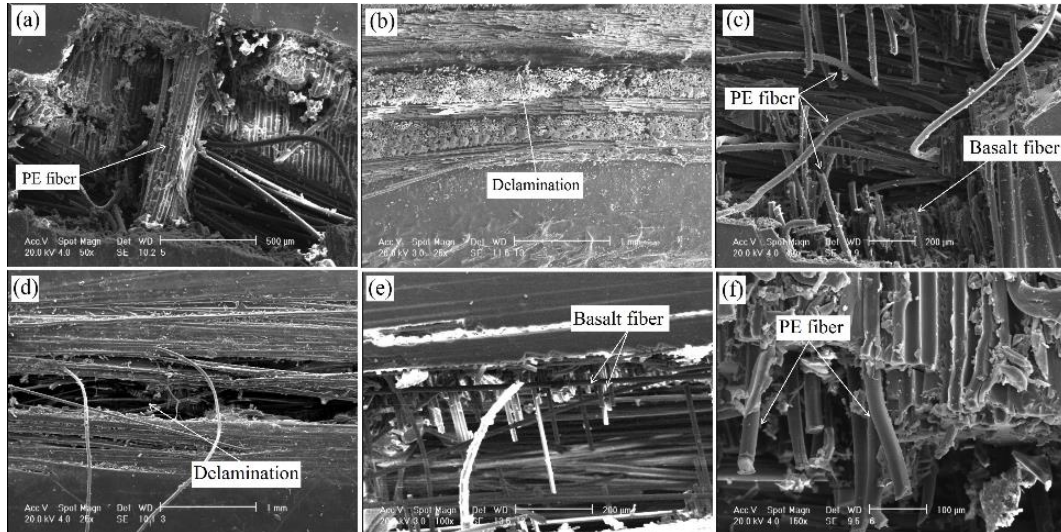
Fig. 3 The fracture surface of (a) Interply2f, (b) Interply1b, (c) Intraply, (d) FGM2f, (e) FGM1f and (f) FGM3f

Table 3 Experimental data obtained from the flexural test applied on the different composites

Sample	Strength (MPa)	Flexural modulus (GPa)	Strength (MPa)	Flexural modulus (GPa)	Strength (MPa)	Flexural modulus (GPa)
	1.3 mm/min		10 mm/min		100 mm/min	
Interply1f	274	9.2	278	8.7	291	6.5
Interply1b	234	7.22	235	7.2	248	5.88
Interply2f	353	10.56	381	9.80	403	9.4
Interply2b	335	8.5	352	9.8	370	9.5
Intraply	282	7.7	296	5.5	313	6
FGM1f	303	8.18	305	7.35	330	8.8
FGM1b	289	8	287	8.44	290	8.1
FGM2f	291	8.23	295	7.40	310	9.41
FGM2b	280	7.92	278	10.04	295	9.55
FGM3f	287	7.54	348	9.34	346	9.4
FGM3b	282	6.37	307	8.3	324	8.1

The experimental data obtained from the bending test for inter-ply, intra-ply and FGM hybrid composites at 1.3, 10 and 100 loading speeds are summarized in Table 3. By looking at the inter-ply hybrid results, it is clear that at all the loading speeds, the samples of Interply2f and Interply2b exhibit higher flexural strength while samples of Interply2f and Interply1f show the highest flexural modulus. The flexural strength of the inter-ply hybrid composites mainly depends on this fact that which fiber is present in the tension and compression side of the specimen (Hancox 1981). The results of Table 3 show that the flexural strength of Interply2f and Interply2b sample is 18-34 percent higher than that of Interply1f and Interply1b samples. This result is due to the difference in the stacking sequence of the specimens and the type of fracture during the bending process. For the Interply2f and Interply2b, the full basalt layers are scattered all over the thickness,

where the basalt fibers which have higher tensile and compressive strength compared to the PE fibers (Akhbari *et al.* 2008), show more resistance to the compressive stress in the upper layers and to the tensile stress in the lower layers. Also, for theInterply2f and Interply2b samples, the PE fiber at the bottom layers was bent in the damage area and prevented its complete collapse (Fig. 3(a)). These results are attributed to the high elongation and ductile nature of the PE fibers (Akhbari *et al.* 2008). In the Interply1f and Interply1b samples, the asymmetry of the fiber type caused a large delamination in the middle section of the thickness (Fig. 3(b)).

For the flexural modulus, a slightly different result is obtained. The results in Table 3 show that at a loading speed of 1.3, samples Interply2f and Interply1f exhibit higher flexural modulus, while at a loading speed of 10 and 100, samples Interply2f and Interply2b show the highest flexural modulus. At bending in standard conditions (loading speed of 1.3), the flexural modulus is a value of the resistance to the deformation of the composite, and is related to the stiffness on the compressive side (Park and Jang 1998). In this case, when the basalt fiber is loaded under compression (samples Interply1f and Interply2f), the highest flexural modulus is obtained. These results are agreement with what was found by Park and Jang (1998), Dong and Davies (2012) and Tehrani *et al.* (2015) who reported that the flexural modulus depends on only the composite rigidity of the compressive side. At loading speeds of 10 and 100, the results have changed to the standard conditions. In these loading speeds, although the basalt fiber-rich layers in the upper side were effective, but the uniform distribution of the two fibers all over the thickness had a greater effect.

The flexural strengths and modulus of the intra-ply hybrid composite are reported in Table 3. In this sample, basalt and PE fibers are mixed in each layer of the composite. Although intra-ply and inter-ply hybrid composites have equal volume ratio of basalt and PE fibers, it is clear that in all loading speeds an intra-ply hybrid laminate exhibit a 16-20 percent lower flexural strength compared to the samples Interply2f and Interply2b. This result is due to the presence of the basalt fiber-rich layers on the tension side (back side) and compression side (front side) of these inter-ply laminates. From the other point of view, at different loading speeds the Intraply sample has a 2-20 percent higher flexural strength compared to samples Interply1f and Interply1b. The results show that the flexural strength of the intra-ply laminate is close to the mean value of the two inter-ply laminates.

The modulus results in Table 3 show that in all of the loading speeds the flexural modulus of the inter-ply hybrid composites is comparable to, or higher than the intra-ply sample. The presence of the basalt fiber-rich layer on the compressive side (front side) of the inter-ply laminate caused resistance to the compressive applied load and consequently a higher flexural modulus is obtained. Fig. 3(c) shows the bottom side of the Intraply sample after failure. As can be seen the basalt fibers are broken as a result of the tension in the lower layers, but the PE fibers are pulled out of the surface by tension. In this sample unlike the Interply2f sample, the load is increased to the point that the PE fibers are completely pulled out of the matrix and ruptured.

Flexural strengths and flexural modulus of the three FGM samples are summarized in Table 3. The results show that at low loading speed, the flexural strength of the FGM specimens were slightly different (up to 6 percent), but with increasing the loading speed, the difference in the flexural strength of these specimens increased. At loading speeds of 10 and 100, the flexural strength of FGM3f specimen was 20 percent higher than the other FGM specimens. This result could be due to the simultaneous presence of a considerable amount of basalt fibers in the top and bottom side of the FGM3f specimen and better reaction of the upper and lower layers of this specimen respectively to the pressure and tensile load. As shown in Figs. 3(d)-(f), the mode of

destruction are matrix cracking, basalt fiber fracture, debonding and rupture of the PE fibers and delamination in the FGM samples.

Comparing the flexural modulus of the FGM specimens with each other shows that at a loading speed of 1.3, the flexural modulus is dependent on the stiffness of the upper layers. Therefore in this case, FGM1f and FGM2f specimens with more basalt fibers in the upper layers have higher flexural modulus, than the other specimens. At loading speeds of 10 and 100, due to the rapid diffusion of the stress and strain along the thickness, other parameters such as the uniform distribution of the fibers along with the thickness and also the stiffness of the lower layers also affect the results. Therefore, in these cases the flexural modulus results change relative to the bending state at the loading speed of 1.3.

The direct comparison between the FGM laminates and other samples which are characterized by the equal volume ratio of basalt and PE fibers, clearly confirms that at all loading speeds the flexural strength of FGM hybrid composites is comparable, or higher than the intra-ply sample. It can be seen that at high loading speeds an FGM3f hybrid laminate exhibits 10-15 percent flexural strength higher than the intra-ply laminate. The FGM hybrid composites show the flexural strength between of the two inter-ply laminates. It can be seen that the FGM samples exhibit a comparable, or higher flexural strength (up to 24-32 percent at different loading speeds) compared to the samples of Interply1f and Interply1b, while these laminates have lower flexural strength (up to 20-28 percent at different loading speeds) compared to samples Interply2f and Interply2b. Comparing the flexural modulus of FGM specimens with the other specimens show that as mentioned above, at a loading speed of 1.3, the rigidity of the upper layers have a significant effect on the flexural modulus. Due to this, the flexural modulus of FGM1 (f and b) and FGM2 (f and b) specimens are 6 percent more than the Intraply specimen, while these specimens have a10-22 percent lower flexural modulus compared to the Interply1f and Interply2f specimens. The results show that at a loading speed of 10 and 100, the flexural modulus of FGM samples is more than the intra-ply and more or equal to the inter-ply samples.

3.1.2 Flexural properties as a function of loading direction

The comparison of the results presented in Table3 show that the direction of the bending load on the upper or lower sides of the different specimens (e.g., Interply1f and Interly1b) has a significant effect on the flexural strength and flexural modulus. It can be seen that when the PE fibers are loaded under tension (samples Interply1f, Interply2f, FGM1f, FGM2f and FGM3f), the highest flexural strength is obtained which is because the excellent bending and elongation properties of the PE fibers eliminated most of the applied flexural energy. The PE fiber is a ductile fiber with high elongation, and it absorbs much tensile energy by fiber pull-out (see Fig. 3(f)) and plastic deformation (Akhbari *et al.* 2008). Also, in standard condition when the basalt fibers are loaded under compression (samples Interply1f, Interply2f, FGM1f, FGM2f and FGM3f), the highest flexural modulus is obtained because the excellent stiffness properties of basalt fibers (Tehrani *et al.* 2015, Nosraty *et al.* 2015) cause the top layers to resist against the flexural load (Fig. 4).

3.1.3 Flexural properties as a function of the loading speed

Figs. 5(a) and (b) show the mean values of the flexural strength and modulus for the inter-ply, intra-ply and FGM laminates at the loading speed of 1.3, 10 and 100. The results indicate that the flexural strength increases approximately for all the specimens by increasing the loading speed from 1.3 (to 10 and 10) to 100 mm/min. These results are in agreement with what was found by
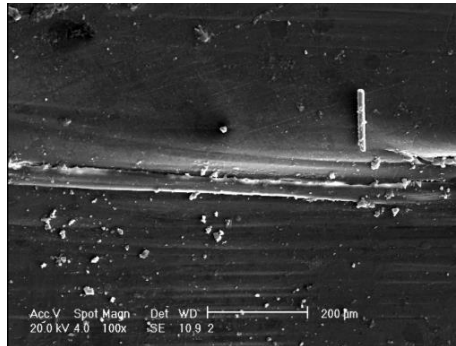
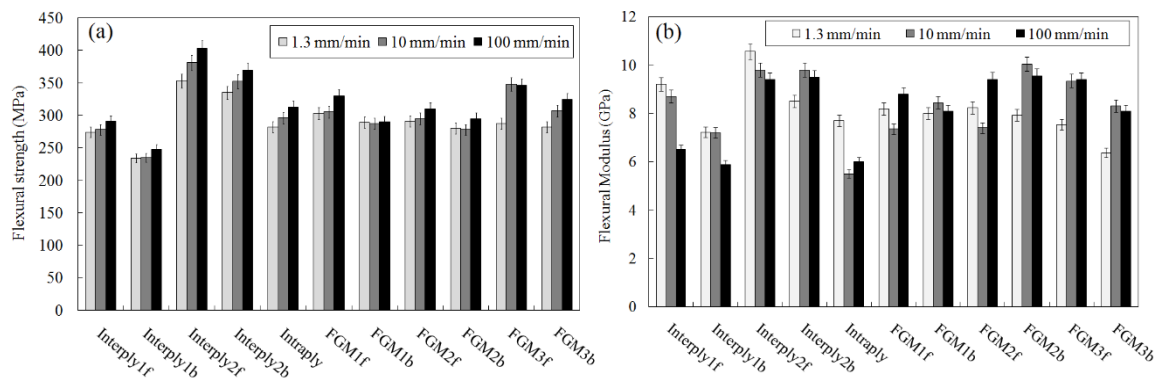Fig. 4 Top surface of the Interply1f sample

Fig. 5 The effect of loading speed on the (a) flexural strength and (b) flexural modulus of the different composites
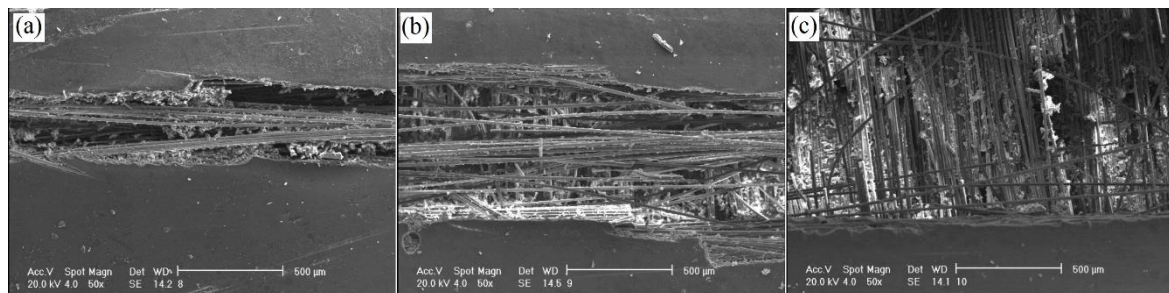

Fig. 6 Bottom surface of the Interply2b sample at loading speeds of (a) 1.3, (b) 10 and (c) 100 mm/min

Tehrani *et al.* (2015) and Okoli (2001). Comparison of the values in Fig. 5(a) shows that the ultimate flexural strength values at 10 mm/min loading speed are 7, 5 and 17 percent higher than those calculated at 1.3 mm/min for the inter-ply, intra-ply and FGM samples, respectively. Also, the ultimate flexural strength values at 100 mm/min loading speed are 12, 10 and 17 percent higher than those calculated at 1.3 mm/min for the inter-ply, intra-ply and FGM samples, respectively. For the above observation, it is important to note that at high crosshead speed, the available time is very small for the failure to occur, therefore the matrix may not properly be able to transfer the load which, leads to more matrix cracking (Figs. 6(a)-(c)) and increase in the

ultimate strength value (Tehrani *et al.* 2015, Okoli 2001). Comparison of the values in Fig. 5(b) shows that the flexural modulus does not have any special trend by increasing the loading speed from 1.3 (to 10 and 10) to 100 mm/min. This result may be due to a change in the fracture mechanism and a change in the sequence of the destruction in samples at different loading speeds (Shokrieh and Omidi 2009).

3.2 Charpy impact properties

The normalized impact absorption energy for the various composites, where the impact was applied on the top and bottom surfaces, is summarized in Fig. 7. It can be seen that depending on the stacking sequence the total impact absorption energy for the inter-ply hybrid composites ranges from 11.64 to 16.16 $J.cm^{-2}$. The absorption energy of the Interply2f sample is 28 percent higher than the Interply1f sample. This discrepancy is due to the different stacking sequence of these two samples. As shown in Fig. 8(a), in the Interply1f sample, six layers of the PE fibers which are easily stretchable (Akhbari *et al.* 2008), are located in the bottom side of the sample therefore the lower layers do not have a reasonable tensile stiffness and the PE fibers in these layers are easily debonded and ruptured. Also, the shear forces in the Interply1f sample, due to the complete asymmetry of the top and bottom layers (and different properties of the basalt fibers in the top layers and the PE fibers in the bottom layers (Akhbari *et al.* 2008, Nosraty *et al. 2015*), create long splitting in the middle of this sample (see Fig. 8(a)). In the Interply2f sample, the presence of basalt fiber-rich layers in the bottom side caused this sample to withstand sudden tensile stresses, less sample degradation, and greater impact resistance (Fig. 8(b)).

Comparing the impact performance of the intra-ply sample with the inter-ply samples shows that the absorption energy of the Intraply sample is 30 percent lower than the Interply2f sample. These results are in agreement with what was found by Wang *et al.* (2008) and Peggoretti *et al.* (2004) for the intra-ply and inter-ply samples. In the intra-ply sample, the simultaneous presence of PE and basalt fibers in each layer and the similarity of all the layers caused all of the layers to have the same tensile (or compressive) strength during the impact process. Therefore, the delamination between the layers in this sample is minimum compared to the inter-ply samples (Wang *et al.* 2008). However, the simultaneous presence of the PE and basalt fibers in each layer caused the composite layers to have less tensile or compressive strength relative to the full basalt layers. During the impact process of the Intraply sample, the PE fiber debonded and ruptured and also the basalt fiber was severely broken (Fig. 8(c)).

As shown in Fig. 7, the FGM composites which were impacted on the top side showed impact absorption energy values in the range of 12.48-13.96 $J.cm^{-2}$, while the least value of 8.57 $J.cm^{-2}$, was obtained for the FGM3b composite which impacted on the bottom side. Comparing the performance of the FGM samples with each other shows that the absorption energy of FGM2f and FGM3f samples was not significantly different. But the absorption energy of the FGM1f sample was 8-10 percent higher than the other FGM samples. This discrepancy may be due to the higher amount of basalt fibers at the top layers of the FGM1f sample and as a result better compressive strength compared to the other samples was obtained. The extent and type of the damages for the FGM samples are illustrated in Figs. 8 (d)-(f). In the FGM1f specimen, the discrepancy of the fiber type in the adjacent layers is smaller than the other FGM specimens; therefore the delamination in this sample is lower than the other FGM samples (Fig. 8(d)). Such as the inter-ply samples for the FGM3f sample, the discrepancy of the fiber type in the outside and inside layers was very high, therefore the delamination significantly increased in this sample, (Fig. 8(f)).
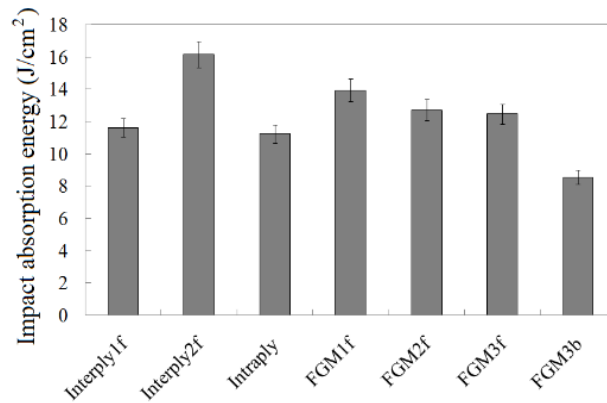
Fig. 7 Normalized impact absorption energy obtained for the various composites
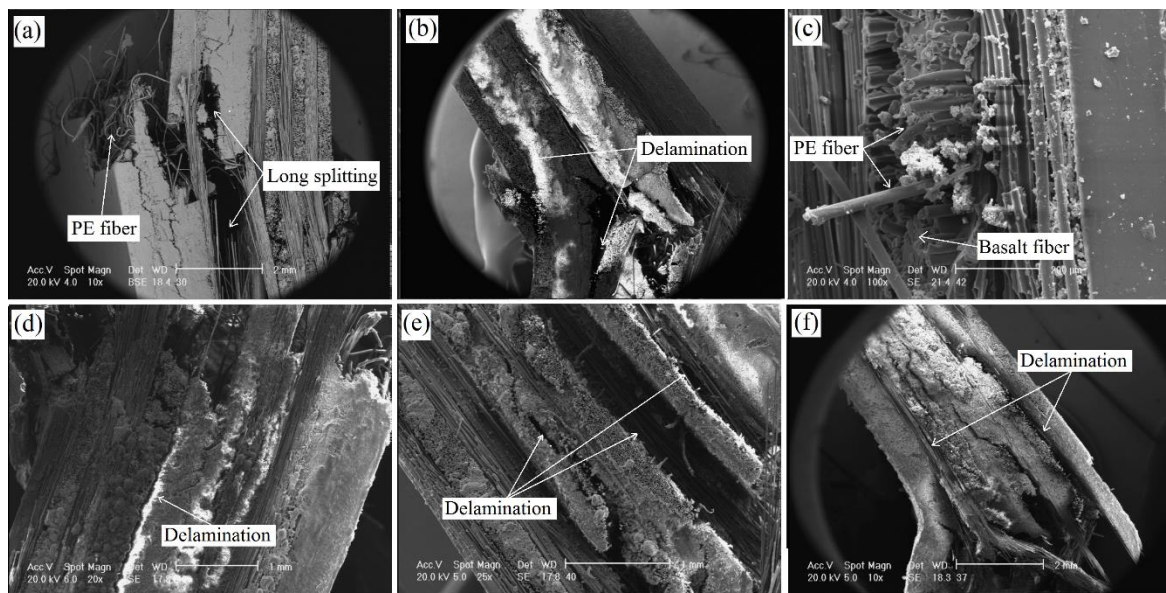

Fig. 8 The fracture surface of the (a) Interply1f, (b) Interply2f, (c) Intraply, (d) FGM1f, (e) FGM2f and (f) FGM3f composites

Comparison the impact results of the FGM samples with the other samples show that the absorption energy of the FGM samples are 10-20 percent higher than the intra-ply sample. This result could be due to the presence of the basalt fibers at the top layers of the FGM samples and consequently better compressive strength of these samples is obtained relative to the intra-ply sample. Also the results presented in Fig. 7 show that the FGM samples have 6-16 percent higher absorption energy compared to the Interply1f sample, while these specimens have a 14-22 percent lower absorption energy compared to the Interply2f sample.

The impact absorption energy of the FGM3b sample is illustrated in Fig. 7. As can be seen in Table 2, the structure of this specimen is similar to the FGM3f sample and only the direction of the applied impact on the top and bottom sides of the samples differs. Comparing the absorption

energy of these samples shows that the FGM3b sample has32 percent lower absorption energy compared to the FGM3f sample. This result is due to the presence of full basalt fiber in the top layer of the FGM3f sample. In the FGM3bsample, the PE fiber-rich layer in the compressive side deflects and deforms easily so that the low impact energy is absorbed by the PE fiber pull-out and fiber/matrix debonding (Akhbari *et al.* 2008). In the FGM3f sample, the PE fibers at the tension side do not act as crack arrestors, while the brittle basalt fibers at the compressive side absorb the initial impact energy and restrict the severity of the impact (Nosraty *et al.* 2015, Onal and Adanur 2019). These results are compatible with what was found by Jang and Lee (1998), who reported that in the FGM composites, the impact absorption energy would be slightly increased when the ductile fibers (glass fibers) were used in the compressive side and the brittle fibers (carbon fiber) were used in the tensile side. The reason for the discrepancy between the results of this study and those of Jang and Lee (1998) is the difference between the type of the fibers and the stacking sequence of the composites used in these two studies.

4. Conclusions

Three types of basalt-PE/epoxy hybrid composites with similar fiber volume fraction were designed and fabricated, namely inter-ply, intra-ply and FGM hybrid composites. Their flexural and charpy impact properties were tested. The results indicate that:
   • The flexural and impact behavior of the hybrid composites changes markedly when the spatial distribution of the reinforcing fibers are altered in the hybrids.
   • With a properly choosing the composition and stacking sequence of the plies, the inter-ply hybrid composites can achieve better flexural strength, flexural modulus and impact absorption energy compared to the intra-ply and FGM composites. Also, the FGM hybrid composites can achieve better flexural and impact properties compared to the intra-ply ones.
   • When the basalt fibers are loaded under compression (samples Interply1f, Interply2f, FGM1f, FGM2f and FGM3f), the highest flexural modulus is obtained.
   • By increasing the loading speed from 1.3 (to 10 and 10) to 100 mm/min, the flexural strength increases and the flexural modulus does not have any special trend. The ultimate flexural strength values at 100 mm/min loading speed are up to 12, 10 and 17 percent higher than those calculated at 1.3 mm/min for inter-ply, intra-ply and FGM samples, respectively.
   • When the basalt fibers are used on the surface side (top and bottom side of the sample), the highest impact absorption energy is obtained.

References

Akhbari, M., Shokrieh, M.M. and Nosraty, H. (2008), "A study on buckling behavior of composite sheet reinforced by hybrid woven fabrics", *Trans. Can. Soc. Mech. Eng.*, **32**, 81-89. https://doi.org/10.1139/tcsme-2008-0006.

Artemenko, S.E. (2003), "Polymer composites materials made from carbon, basalt and glass fibers, structures and properties", *Fibre Chem.*, **35**, 226-229. https://doi.org/10.1139/tcsme-2008-0006.

ArySubagia, I.D.G. and Kim, Y.A. (2013), "A study on flexural properties of carbon-basalt/epoxy hybrid composites", *J. Mech. Sci. Tech.*, **27**, 987-992. https://doi.org/10.1007/s12206-013-0209-5.

ASTM D256-10 (2018), Standard Test Methods for Determining the Izod Pendulum Impact Resistance of Plastics.

ASTM D790-03 (2003), Standard Test Method for Flexural Properties of Unreinforced and Reinforced Plastics and Electrical Insulating Materials.

Azizi, H. and Eslami-Farsani, R. (2021), "Study of mechanical properties of basalt fibers/epoxy composites containing silane-modified nanozirconia", *J. Indus. Text.*, **51**(4), 643-649. https://doi.org/10.1177/1528083719887530.

Bafekrpour, E., Yang, C., Natali, M. and Fox, B. (2013), "Functionally graded carbon nanofiber/phenolic nano composites and their mechanical properties", *Compos. Part A: Appl. Sci. Manuf.*, **54**, 124-134. https://doi.org/10.1016/j.compositesa.2013.07.009.

Bharti, I., Gupta, N. and Gupta, K.M. (2013), "Novel applications of functionally graded nano, optoelectronic and thermoelectric materials", *Int. J. Mater., Mech. Manuf.*, **3**, 221-224. https://doi.org/10.7763/IJMMM.2013.V1.47.

Caminero, M.A., Garcia-Moreno, I. and Rodriguez, G.P. (2018), "Experimental study of the influence of thickness and ply-stacking sequence on the compression after impact strength of carbon fibre reinforced epoxy laminates", *Polym. Test.*, **66**, 360-370. https://doi.org/10.1016/j.polymertesting.2018.02.009.

Dong, C. and Davies, I.J. (2012), "Optimal design for the flexural behaviour of glass and carbon fibre reinforced polymer hybrid composites", *Mater. Des.*, **37**, 450-457. https://doi.org/10.1016/j.matdes.2012.01.021.

Hancox, N.L. (1981), *Fibre Composite Hybrid Materials*, Applied Science Publishers Ltd, London.

Huang, Z.M., Wang, Q. and Ramakrishna, S. (2002), "Tensile behaviour of functionally graded braided carbon fibre/epoxy composite Material", *Polym. Polym. Compos.*, **10**, 307-314. https://doi.org/10.1177/096739110201000406.

Jang, J. and Lee, C. (1998), "Performance improvement of GF/CF functionally gradient hybrid composites", *Polym. Test.*, **17**, 383-394. https://doi.org/10.1016/S0142-9418(97)00064-0.

Kim, S.H., Heo, Y.J. and Park, S.J. (2019), "Ozonization of SWCNTs on thermal/mechanical properties of basalt fiber-reinforced composites", *Steel Compos. Struct.*, **31**, 517-527. https://doi.org/10.12989/scs.2019.31.5.517.

Lee, N.J., Jang, J., Park, M. and Choe, C.R. (1997), "Characterization of functionally gradient epoxy/carbon fiber composite prepared under centrifugal force", *J. Mater. Sci.*, **32**, 2013-2020. https://doi.org/10.1023/A:1018502201000.

Nosraty, H., Tehrani-Dehkordi, M., Shokrieh, M.M. and Minak, G. (2015), "Intraply hybrid composites based on basalt and nylon woven fabrics: tensile and compressive properties", *Iran. J. Mater. Sci. Eng.*, **12**, 1-11. https://doi.org/10.22068/ijmse.12.1.1.

Okoli, I. (2001), "The effect of strain rate and failure modes on the failure energy of fiber reinforced composites", *Compos. Struct.*, **54**, 299-303. https://doi.org/10.1016/S0263-8223(01)00101-5.

Onal, L. and Adanur, S. (2019), "Effect of stacking sequence on the mechanical properties of glass-carbon hybrid composites before and after impact", *J. Indus. Text.*, **31**, 255-271. https://doi.org/10.1106/152808302028713.

Özbek, O., Bozkurt, O.Y. and Erkliğ, A. (2019), "An experimental study on intraply fiber hybridization of filament wound composite pipes subjected to quasi-static compression loading", *Polym. Test.*, **79**, 1-9. https://doi.org/10.1016/j.polymertesting.2019.106082.

Park, R. and Jang, J. (1998), "The effect of hybridization on the mechanical performance of aramid/polyethylene intraply fabric composites", *Compos. Sci. Tech.*, **58**, 1621-1628. https://doi.org/10.1016/S0266-3538(97)00228-5.

Pegoretti, A., Fabbri, E., Migliaresi, C. and Pilati, F. (2004), "Intraply and interplay hybrid composites based on E-glass and poly (vinyl alcohol) woven fabrics: tensile and impact properties", *Polym. Inter.*, **53**, 1290-1297. https://doi.org/10.1002/pi.1514.

Rajak, D., Pagar, D.D., Menezes, E.L. and Linul, E. (2019), "Fiber-reinforced polymer composites: manufacturing, properties, and applications", *Polym.*, **11**, 1667. https://doi.org/10.3390/polym11101667.

Shokrieh, M.M. and Omidi, M.J. (2009), "Compressive response of glass-fiber reinforced polymeric composites to increasing compressive strain rates", *Compos. Struct.*, **89**, 517-523. https://doi.org/10.1016/j.compstruct.2008.11.006.

Sun, X. and Hallett, S. (2017), "Barely visible impact damage in scaled composite laminates: Experiments and numerical simulations", *Int. J. Impact Eng.*, **109**, 178-195. https://doi.org/10.1016/j.ijimpeng.2017.06.008.

Tehrani-Dehkordi, M., Nosraty, H. and Rajabzadeh, M.H. (2015), "Effects of plies stacking sequence and fiber volume ratio on flexural properties of basalt/nylon-epoxy hybrid composites", *Fiber. Polym.*, **16**, 918-925. https://doi.org/10.1007/s12221-015-0918-8.

Tehrani-Dehkordi, M., Nosraty, H., Shokrieh, M.M., Minak, G. and Ghelli, D. (2010), "Low velocity impact properties of intraply hybrid composites based on basalt and nylon woven fabrics", *Mater. Des.*, **31**, 3835-3844. https://doi.org/10.1016/j.matdes.2010.03.033.

Thomas, B. and Roy, T. (2016), "Vibration analysis of functionally graded carbon nanotube-reinforced composite shell structures", *Acta Mechanica*, **227**, 581-599. https://doi.org/10.1007/s00707-015-1479-z.

Wang, X., Hu, B., Feng, Y., Liang, F., Mo, J., Xiong, J. and Qiu, Y. (2008), "Low velocity impact properties of 3D woven basalt/aramid hybrid composites", *Compos. Sci. Tech.*, **68**, 444-450. https://doi.org/10.1016/j.compscitech.2007.06.016.

PF